

Noise Properties of a Josephson Parametric Oscillator

Gopika Lakshmi Bhai^{1,2,*}, Hiroto Mukai^{1,2}, Tsuyoshi Yamamoto,^{3,4} and Jaw-Shen Tsai^{1,2,3,†}

¹*Graduate School of Science, Tokyo University of Science, 1-3 Kagurazaka, Shinjuku, Tokyo 162-0825, Japan*

²*RIKEN Center for Quantum Computing (RQC), 2-1 Hirosawa, Wako, Saitama 351-0198, Japan*

³*Research Institute for Science and Technology, Tokyo University of Science, 1-3 Kagurazaka, Shinjuku-ku, Tokyo 162-8601, Japan*

⁴*Secure System Platform Research Laboratories, NEC Corporation, Kawasaki, Kanagawa 211-0011, Japan*

(Received 19 August 2022; revised 25 October 2022; accepted 8 December 2022; published 25 January 2023)

We perform noise spectroscopy of a Josephson parametric oscillator (JPO) by implementing a microwave homodyne interferometric measurement scheme. We observe the fluctuations in the self-oscillating output field of the JPO for a long 10-s time interval in a single-shot measurement and characterize the phase and amplitude noise. Furthermore, we investigate the effects of the pump strength on the output noise power spectra of the JPO. We find strong fluctuations in the phase with a $1/f^2$ characteristic in the phase noise power spectrum, which are suppressed by increasing the pump strength.

DOI: 10.1103/PhysRevApplied.19.014065

I. INTRODUCTION

The study of noise in physical systems has a long history [1]. The measurement and performance aspects of the physical systems have long been considered to be limited by noise [2–5]. Various studies have been done extensively to understand the noise sources and the possibility of evading noise [6–11]. However, evading the intrinsic noise of a physical system is highly challenging and is a fundamental limitation [12–14]. Recently, several advances have led to a renewed interest in the characterization and mitigation of noise in the field of circuit quantum electrodynamics (cQED) [11,15–17]—one of the most promising candidates in quantum computing and quantum information processing [18–20]. The ongoing quest to build a quantum computer has intensified the efforts to study noise in qubits [11,15,16]—the basic building blocks of a quantum computer. However, the noise properties of other essential components used for the readout of the qubit, such as a Josephson parametric amplifier (JPA) or Josephson parametric oscillator (JPO), are rarely explored.

A typical cQED measurement network operates at frequencies of a few gigahertz and a temperature of around 10 mK. Quantum devices such as qubits are commonly read out at a few photon regimes to protect from measurement backaction [11,21,22]. Low noise amplification of the signal is a practical need for detecting weak photons from quantum devices operating in the microwave

regime. A JPA, a typical parametric device consisting of a superconducting resonator integrated with Josephson elements [23–27], overcomes this obstacle by effectively amplifying the signal by adding a minimum noise allowed by the fundamental law of quantum mechanics [14,28]. These devices have become an essential component of the readout chain since they attain quantum-limited amplification by high-frequency modulation of the inductance of the nonlinear Josephson element [26,29,30]. When the modulation amplitude exceeds the instability threshold, self-sustained oscillations start to build up [31], and it works as an oscillator—a Josephson parametric oscillator [32–34]. Due to the new accessible parameter regimes as a consequence of the strong nonlinear properties of JPOs, notable studies have been done demonstrating the generation of squeezed states [35,36], two-mode entanglement [36], cat state engineering [37–40], high-fidelity qubit readout [32,33,41], etc. Nonetheless, the study of the noise properties of JPOs is left unaddressed.

JPOs, like any other oscillators, have ubiquitous noise properties, which give rise to a finite oscillation linewidth typically ranging from a few kilohertz to hertz depending on the operating parameters [34,42–45]. Several unifying theories explain the noise characteristics of an oscillator [46–48]. Over the last few decades, various experimental and theoretical studies in the optical domain have investigated the noise properties of parametric oscillators and lasers [49–53]. Noise spectroscopic studies in the optics field show the limiting factor of the finite linewidth of lasers [13,54] described by the Schawlow-Townes limit [51]. These theories and experimental observations

*gopika.lakshmibhai@gmail.com

†tsai@riken.jp

shed light on investigating the noise properties of JPOs in superconducting circuit systems, where a detailed study of the noise properties of JPOs is yet to be conducted.

In this work, we present an experimental study of the noise characterization of a JPO pumped above its parametric threshold, where the phase coherence of the output photons from the oscillator is investigated. We perform the spectral analysis of noise in the phase and amplitude quadrature at low frequencies and explore the possible noise sources in the JPO.

II. EXPERIMENTAL SETUP

Our device consists of a $\lambda/4$ resonator made with a segment of coplanar waveguide (CPW) terminated by a dc superconducting quantum interference device (SQUID) [26]. The CPW resonator is fabricated by etching out the sputtered niobium on a silicon wafer [55]. The Josephson junctions are then made by standard double-angle shadow evaporation of aluminum [Figs. 1(b) and 1(c)]. The presence of the SQUID makes the resonance frequency of the resonator tunable by a variable Josephson inductance L_J , which follows the relation $L_J = \Phi_0/(4\pi I_c |\cos(\pi\Phi_{dc}/\Phi_0)|)$. Here, I_c is the critical current through the junction, Φ_{dc} is the dc magnetic flux through the SQUID, and Φ_0 is the flux quantum. By changing the flux through the dc SQUID Φ_{dc} , the Josephson inductance can be varied.

An input signal and a pump signal are applied to the device through attenuated lines with filters to the respective ports on the chip. On-chip dc bias is applied through the same pump line using a bias tee. The measurements of the device are carried out in a cryogenic environment using a dilution refrigerator at a base temperature of 10 mK [Fig. 1(a)]. The output signal from the device is routed through a microwave filter, circulator, and isolator, which is amplified using a high-electron-mobility transistor (HEMT) at 4 K. The output signal is then further amplified at room temperature (R.T) using R.T amplifiers.

At first, we characterize the system dynamics by scanning the resonator frequency dependence on the applied magnetic flux using a dc source. A weak probe signal is coupled to the cavity through a circulator in the mixing chamber, and the output from the device is analyzed using a vector network analyzer by measuring the complex reflection coefficient S_{11} . The bare resonator frequency in the absence of flux is found to be $\omega_r/2\pi = 6.239$ GHz. The estimated critical current for each Josephson junction is $1.89 \mu\text{A}$, which is obtained from fitting the resonator spectrum. The external and internal cavity losses are found to be $\kappa_{\text{ext}}/2\pi = 11$ MHz and $\kappa_{\text{int}}/2\pi = 0.3$ MHz at a flux bias of $\Phi_{dc}/\Phi_0 = 0.35$ with a resonance frequency of $\omega_r/2\pi = 5.94$ GHz. To further characterize the operational properties of the JPA, we apply a pump signal with a

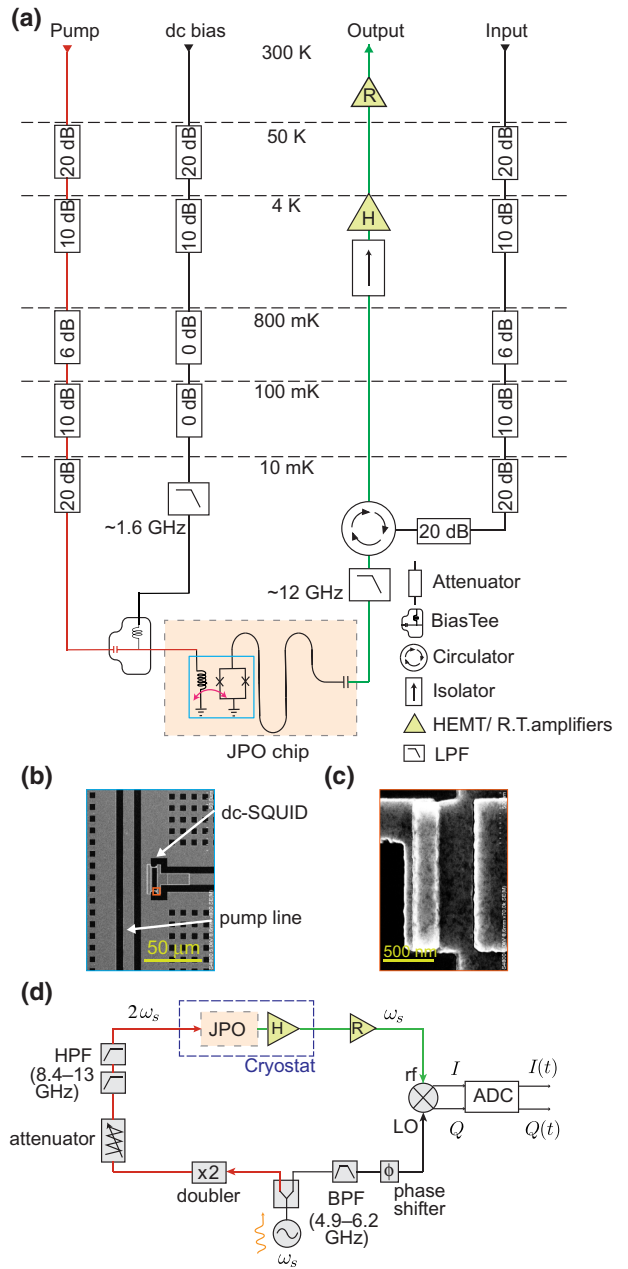


FIG. 1. (a) Schematic illustration of the cryogenic microwave measurement setup. (b) Scanning electron microscope (SEM) image showing the SQUID consisting of two parallel-connected Josephson junctions. The SQUID made of aluminum is galvanically coupled to the central conductor of the CPW patterned on a niobium film, which is deposited on a silicon substrate through sputtering. There are ground plane holes to pin the trapped flux on the chip. (c) SEM image showing the Josephson junction made of Al/AlO_x/Al. (d) Microwave interferometric setup to measure the phase noise of the JPO: input lines are color-coded with the cryogenic circuit lines in (a), which describes the signal flow.

frequency $\omega_p \approx 2\omega_r$, where ω_r is the resonator frequency at a specific flux point. The pump photons interact with the incoming signal photons and generate an amplified

signal with an approximate gain of 20 dB at pump power $P_p = -63.4$ dBm.

To investigate photon generation, we apply the pump signal at twice the resonance frequency in the absence of the input signal and examine the output from the JPA by increasing the pump power P_p . As the pump power increases beyond the parametric instability threshold, self-sustained oscillations build up exponentially in time inside the cavity. This can be understood as a second-order phase transition from a ground state below the threshold to an excited state above the threshold [56,57]. In order to investigate the region of parametric instability, we choose a flux bias point on the flux-frequency curve at $\Phi_{dc}/\Phi_0 = 0.35$, and we span the parametric plane by varying the pump-resonator detuning $\delta = |\omega_r - \omega_p/2|$ and pump power P_p , as shown in Fig. 2(a). Here we see the regime of parametric oscillation throughout a well-defined interval of detuning δ . The asymmetry of the parametric plane can be due to the pump-induced nonlinearity [33]. Figure 2(b) shows the output power from the JPO detected with a spectrum analyzer as a function of applied pump power P_p from a microwave source with $\omega_p/2\pi = 2 \times 5.94$ GHz. The power levels described are referred to the corresponding ports on the chip. As the pump power increases, crossing the threshold, the output power from the JPO increases exponentially, indicating the onset of parametric oscillation. In this above-threshold region, where the pump power is sufficiently strong, the nonlinearity of the system leads to bistability in the effective potential of the JPO field, as shown in the inset of Fig. 2(b). As a consequence of the bistability, the output oscillating field of the JPO has two stable states with a well-defined phase of either 0 or π [32,58].

Next, we measure the noise properties of the JPO operated at a pump frequency of $\omega_p/2\pi = 2 \times 5.94$ GHz at a fixed flux bias $\Phi_{dc}/\Phi_0 = 0.35$. The measurement setup is shown in Fig. 1(d). We use a homodyne interferometric measurement scheme where the output frequency of the JPO is mixed with a local oscillator at the same frequency to extract the phase and amplitude components of the signal using an *I*-*Q* mixer. A microwave source at a frequency the same as the JPO output signal frequency ω_s is split into two equal signals using a microwave splitter. One split signal is fed to the local oscillator of the *I*-*Q* mixer through a band-pass filter and a phase shifter, whereas the other equally divided signal is connected to the JPO pump port by doubling the frequency using a frequency doubler. This pump signal is connected to a tunable attenuator to modulate the pump power. A series of carefully chosen high-pass and band-pass filters are connected to the pump and local oscillator signal path to filter out signals at unwanted frequencies. The transmitted output from the JPO is amplified with the HEMT and R.T amplifiers, which is then fed to the rf port of the *I*-*Q* mixer. The *I* and *Q* signals from the *I*-*Q* mixer are connected

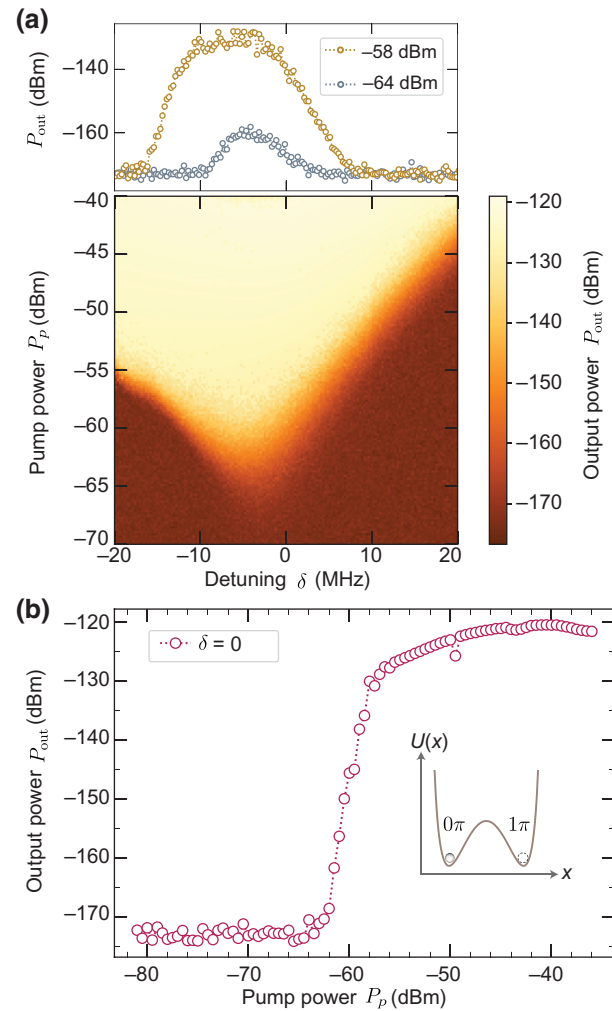


FIG. 2. (a) Span of the parametric regime of the JPO. The output power from the JPO (in the absence of a probe signal) is plotted against the pump power measured by changing the detuning δ between the resonator and pump frequencies. The top panel shows the cross section at two fixed pump powers. (b) Output power from the JPO as a function of the applied pump power (P_p). The static resonance frequency of the JPO is 5.94 GHz, at which the phase noise measurement of the JPO is carried out. The inset shows a qualitative picture of the bistable potential of the JPO, which has two stable minima corresponding to the oscillating states of 0π and 1π [32].

to the two channels of a 14-bit Keysight digitizer with an onboard field-programmable gate array (FPGA) for real-time sequencing. For the low-frequency phase noise measurements, the default sampling rate of the digitizer is reduced to 1 MSa/s before channeling the signal to data acquisition. Using the custom FPGA image, this reduction in the sampling rate is made with three-stage finite impulse response filters with decimation of 1/5, 1/4, and 1/25 in each step to obtain the desired sampling rate. The phase shifter in the local oscillator signal path is tuned to calibrate the offset between the *I* and *Q* signals due to the

mixer imperfection and to utilize the digitizer's maximum dynamic range. We then observe this digitized data in real time for a long period of 10 s in a single shot. The I and Q signals are observed to be fluctuating about their mean. To quantify the JPO noise from these data, we first carry out spectral noise analysis [59,60] of these digitized I and Q signals by studying the spectral domain noise covariance matrix $S(\nu)$, defined by

$$\langle \delta\xi(\nu)\delta\xi^\dagger(\nu') \rangle = S(\nu)\delta(\nu - \nu'), \quad (1)$$

$$S(\nu) = \begin{pmatrix} S_{II}(\nu) & S_{IQ}(\nu) \\ S_{IQ}^*(\nu) & S_{QQ}(\nu) \end{pmatrix}. \quad (2)$$

Here, $\delta\xi(\nu)$ is the Fourier transform of the fluctuation in the I and Q signals about their mean, represented by $\delta\xi(t) = [\delta I(t), \delta Q(t)]^T$. Its Hermitian conjugate is given by $\delta\xi^\dagger(\nu)$. The diagonal terms $S_{II}(\nu)$ and $S_{QQ}(\nu)$ in the matrix represent the auto power spectra. The off-diagonal element $S_{IQ}(\nu)$ represents the cross power spectra and $S_{IQ}^*(\nu)$ represents its complex conjugate.

For a fixed pump power and frequency, the I and Q signals are recorded continuously for 10 s. These time-trace data are then transferred to a CPU for further analysis. We calculate the spectral density using Welch's method [61]. As described in Ref. [59], we find that the imaginary part of S_{IQ} is negligible, and the matrix can be diagonalized with an ordinary rotation $O(\nu)$ applied to $\text{Re}[S(\nu)]$. Thus by diagonalizing it for all the frequencies, we obtain the eigenvalues as

$$O^T(\nu)\text{Re}[S(\nu)]O(\nu) = \begin{pmatrix} S_{aa}(\nu) & 0 \\ 0 & S_{bb}(\nu) \end{pmatrix}. \quad (3)$$

Here S_{aa} and S_{bb} represent the noise spectra in phase and amplitude quadrature. The measurements are repeated for different pump powers. The phase and amplitude power spectrum for each pump power is averaged five times. The HEMT noise floor and the measurement system noise floors are measured to ensure an adequate signal-to-noise ratio for our measurements.

III. RESULTS AND DISCUSSION

Figure 3(a) shows the phase noise power spectra of the JPO for different pump powers P_p ranging from -64 to -52 dBm, measured at a pump frequency of $\omega_p/2\pi = 2 \times 5.94$ GHz. At low frequencies, the phase noise spectra show a flat response, roll-off with a $1/f^2$ trend, and become white noise at higher frequencies. We note that the dip in the spectra at the highest frequency is due to the anti-aliasing filter. We can see that the phase noise is highly affected by the change in the pump power. When we gradually increase the pump power, we see suppression of phase noise in the $1/f^2$ characteristic region as the total noise envelope moves down to lower frequencies. On

the contrary, the amplitude noise power spectra of the JPO in Fig. 3(b) are observed to be much lower than the phase noise spectra and are dominated by the HEMT noise floor except for a $1/f$ knee at lower frequencies contributed by the electronics. Within the range of our measurement sensitivity, amplitude noise shows no significant variation with the change in the pump power. The multiple peaks in the spectrum from 50 Hz and its harmonics are an artifact of power grid poisoning [62], which could be eliminated using appropriate filters [63].

Figure 3(c) shows the trajectory of the JPO output in the I quadrature for two different pump powers of $P_p = -62$ dBm and $P_p = -58$ dBm, cropped from a 10-s-long time trace recorded in a single-shot measurement. We see that the signal is purely random, with discrete switching between two favorable states. It follows the typical characteristics of a random telegraphic noise which contribute to a Lorentzian noise spectrum in the frequency domain [64]. In JPOs, the switching between two states originates from the presence of a bistable potential whose minima correspond to 0π and 1π states [32]. We observe multiple flips between 0π and 1π states during an interval of 10 s.

For further analysis, we fit the noise spectra shown in Fig. 3(a) with a generalized Lorentzian [64,65] given by $S(f) = A\Gamma_r/(\pi^2 f^2 + \Gamma_r^2) + B$, where Γ_r , A , and B are fitting parameters. Γ_r is the corner frequency, which is proportional to the interstate switching rate between $0\pi \rightarrow 1\pi$ and $1\pi \rightarrow 0\pi$ transitions [64]. We also define a corner frequency f_w at which the $1/f^2$ region rolls down to a white noise. Frequency f_w is evaluated from a $1/f^2$ fit where it meets the white noise floor. These two corner frequencies for different pump powers are plotted in Fig. 3(d). For the lowest measured pump power, the switching rate is the highest. As the pump power gradually increases, the output oscillating field stays pinned to one of the two states for longer periods; as a result, the switching rate decreases. This can be understood from the theoretical description in Ref. [32]. The barrier height of the bistable potential rises with the increase in the pump strength, which reduces the transition events between the two states, and the switching rate falls off exponentially [66,67]. We also note that the corner frequency f_w decreases exponentially with the pump power. For $P_p > -58$ dBm, extracting Γ_r from the Lorentzian fit is nonviable since our sampling time interval is limited to 10 s. Hence, we count the number of switching events from the time-domain data and estimate Γ_r . The open triangles in Fig. 3(d) show the estimated Γ_r for these powers. At these pump powers, the switching events are rare, and the oscillator field stays in one of its states for an extended period.

The switching between the bistable states could be a manifestation of a variety of mechanisms, including quantum fluctuation, thermal activation, or quantum activation [42,53,68]. Further studies of the dynamic evolution of the oscillation output states of the JPO and the characteristic

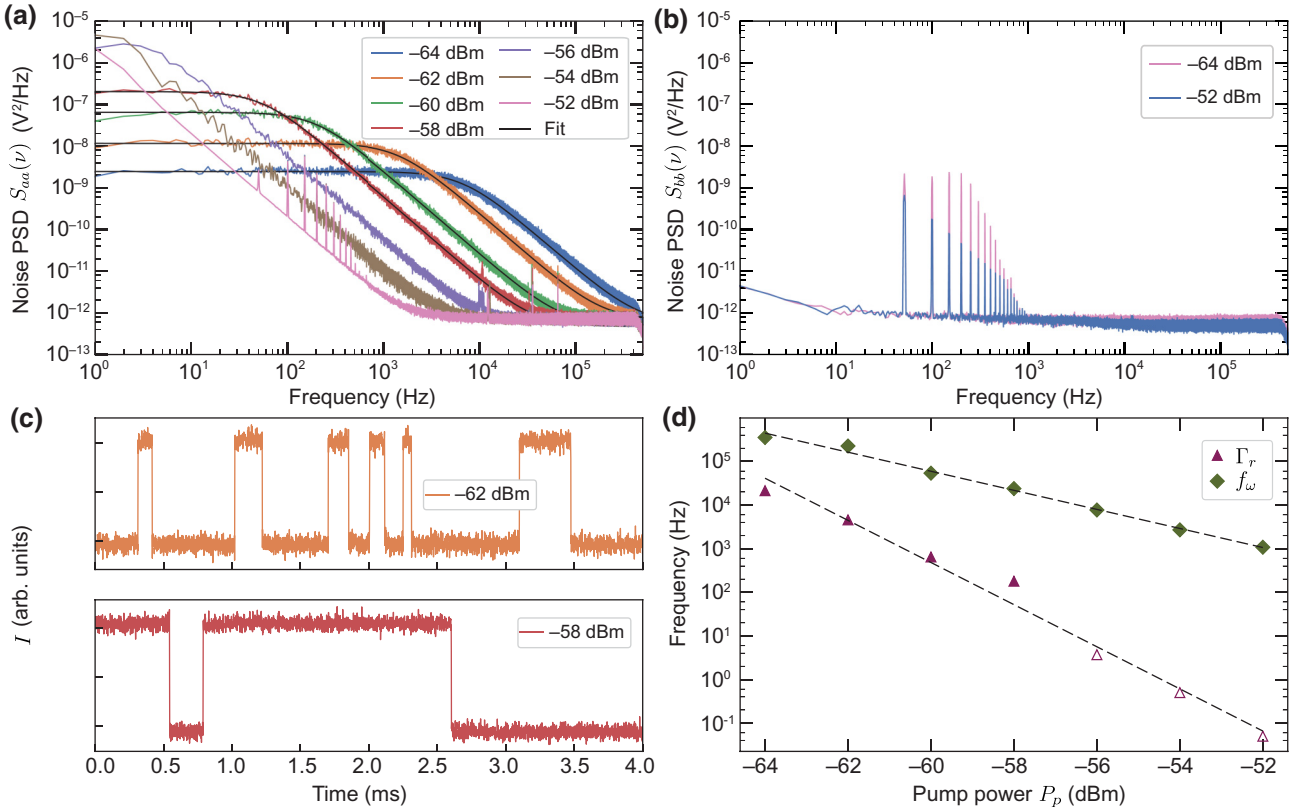


FIG. 3. (a) Noise power spectral density (PSD) in the phase quadrature $S_{aa}(\nu)$ for different pump powers at a fixed pump frequency $\omega_p/2\pi = 2 \times 5.94$ GHz. The solid black line shows the Lorentzian fit to the data. (b) Noise PSD in the amplitude quadrature $S_{bb}(\nu)$ for two distinct pump powers. (c) Trajectory of the I quadrature as a function of time, which is cropped from the full time trace for two different pump powers. (d) Pump power dependence of corner frequencies Γ_r and f_w . Here, Γ_r refers to $1/f^2$ roll-off and f_w refers to the roll-off from $1/f^2$ to a white noise. Values of Γ_r shown as filled triangles are calculated from the Lorentzian fit, and those shown as open triangles are estimated from the time-domain data by counting the number of switching events. Black dashed lines show the exponential fits.

dependence of switching rate on the operating temperature would unravel the nature of this interstate transition [69]. More detailed theoretical studies of the switching rate specific to our nonlinear dynamical system and further experimental investigation of the dynamics of the JPO are the subject of our future work. Furthermore, the present system provides a platform to study and investigate the effects of a weak injection locking signal [70], which is generally known to suppress the phase noise in self-sustained oscillators.

IV. CONCLUSION

In conclusion, we carry out noise spectroscopy of a JPO with a microwave homodyne interferometric measurement scheme. We discuss the analysis method to separate the noise power spectrum in the phase and amplitude quadrature. The extracted amplitude noise power spectra are much below the phase noise power spectra. The phase noise power spectra show signatures of random telegraphic

noise due to the interstate transition of the output oscillating field between the two stable states of the JPO. This random telegraphic noise contributes to a $1/f^2$ noise characteristic to the phase noise power spectra. We study this behavior by increasing the pump power and observe a significant reduction in the switching rate and suppression in the phase noise. Our noise analysis gives deeper insights into the dynamics and the noise characteristics of the JPO.

ACKNOWLEDGMENTS

We are grateful to V. Sudhir, J. Gao, and M. I. Dykman for their thoughtful comments on this research. We acknowledge fruitful discussions with E. Rubiola, P. Patil, R. Wang, S. Shirai, Y. Zhou, S. Kwon, K. Koshino, F. Yoshihara, and Y. Urade. We thank K. Nittoh for support in fabrication. We also thank K. Kikuchi for the technical support from Keysight. This research work is supported in part by JST Moonshot R&D (Grant No. JPMJMS2067), JST CREST (Grants No. JPMJCR1676 and No. JPMJCR1775), and New Energy and Industrial

Technology Development Organization (NEDO) (Grant No. JPNP16007). H.M. is supported by RIKEN SPR project.

-
- [1] S. Kogan, *Electronic Noise and Fluctuations in Solids* (Cambridge University Press, Cambridge, UK, 1996).
- [2] J. B. Johnson, Thermal agitation of electricity in conductors, *Phys. Rev.* **32**, 97 (1928).
- [3] V. Radeka, $1/|f|$ noise in physical measurements, *IEEE Trans. Nucl. Sci.* **16**, 17 (1969).
- [4] R. McDermott, Materials origins of decoherence in superconducting qubits, *IEEE Trans. Appl. Supercond.* **19**, 2 (2009).
- [5] P. Dutta and P. Horn, Low-frequency fluctuations in solids: $1/f$ noise, *Rev. Mod. Phys.* **53**, 497 (1981).
- [6] E. Ivanov and M. Tobar, “Real time” noise measurements with sensitivity exceeding the standard thermal noise limit, *IEEE Trans. Ultrason. Ferroelectr. Freq. Control* **49**, 1160 (2002).
- [7] J. A. Schreier, A. A. Houck, J. Koch, D. I. Schuster, B. R. Johnson, J. M. Chow, J. M. Gambetta, J. Majer, L. Frunzio, M. H. Devoret, S. M. Girvin, and R. J. Schoelkopf, Suppressing charge noise decoherence in superconducting charge qubits, *Phys. Rev. B* **77**, 180502 (2008).
- [8] D. Greywall, B. Yurke, P. Busch, A. Pargellis, and R. Willett, Evading Amplifier Noise in Nonlinear Oscillators, *Phys. Rev. Lett.* **72**, 2992 (1994).
- [9] A. Shnirman, G. Schön, I. Martin, and Y. Makhlin, Low- and High-Frequency Noise from Coherent Two-Level Systems, *Phys. Rev. Lett.* **94**, 127002 (2005).
- [10] V. Giovannetti, S. Lloyd, and L. Maccone, Quantum-enhanced measurements: beating the standard quantum limit, *Science* **306**, 1330 (2004).
- [11] A. A. Clerk, M. H. Devoret, S. M. Girvin, F. Marquardt, and R. J. Schoelkopf, Introduction to quantum noise, measurement, and amplification, *Rev. Mod. Phys.* **82**, 1155 (2010).
- [12] H. Heffner, The fundamental noise limit of linear amplifiers, *Proc. IRE* **50**, 1604 (1962).
- [13] P. Goldberg, P. W. Milonni, and B. Sundaram, Theory of the fundamental laser linewidth, *Phys. Rev. A* **44**, 1969 (1991).
- [14] C. M. Caves, Quantum limits on noise in linear amplifiers, *Phys. Rev. D* **26**, 1817 (1982).
- [15] P. Krantz, M. Kjaergaard, F. Yan, T. P. Orlando, S. Gustavsson, and W. D. Oliver, A quantum engineer’s guide to superconducting qubits, *Appl. Phys. Rev.* **6**, 021318 (2019).
- [16] I. Siddiqi, Engineering high-coherence superconducting qubits, *Nat. Rev. Mat.* **6**, 875 (2021).
- [17] E. Paladino, Y. Galperin, G. Falci, and B. Altshuler, $1/f$ noise: Implications for solid-state quantum information, *Rev. Mod. Phys.* **86**, 361 (2014).
- [18] S. Kwon, A. Tomonaga, G. Lakshmi Bhai, S. J. Devitt, and J.-S. Tsai, Gate-based superconducting quantum computing, *J. Appl. Phys.* **129**, 041102 (2021).
- [19] X. Gu, A. F. Kockum, A. Miranowicz, Y.-x. Liu, and F. Nori, Microwave photonics with superconducting quantum circuits, *Phys. Rep.* **718**, 1 (2017).
- [20] M. H. Devoret and J. M. Martinis, Implementing qubits with superconducting integrated circuits, *Quantum Inf. Process.* **3**, 163 (2004).
- [21] A. Blais, A. L. Grimsmo, S. M. Girvin, and A. Wallraff, Circuit quantum electrodynamics, *Rev. Mod. Phys.* **93**, 025005 (2021).
- [22] J. Gambetta, A. Blais, D. I. Schuster, A. Wallraff, L. Frunzio, J. Majer, M. H. Devoret, S. M. Girvin, and R. J. Schoelkopf, Qubit-photon interactions in a cavity: Measurement-induced dephasing and number splitting, *Phys. Rev. A* **74**, 042318 (2006).
- [23] B. Yurke, P. Kaminsky, R. Miller, E. Whittaker, A. Smith, A. Silver, and R. Simon, Observation of 4.2-K Equilibrium-Noise Squeezing via a Josephson-Parametric Amplifier, *Phys. Rev. Lett.* **60**, 764 (1988).
- [24] A. Roy and M. Devoret, Quantum-limited parametric amplification with Josephson circuits in the regime of pump depletion, *Phys. Rev. B* **98**, 045405 (2018).
- [25] A. Eddins, J. Kreikebaum, D. Toyli, E. Levenson-Falk, A. Dove, W. Livingston, B. Levitan, L. Goria, A. Clerk, and I. Siddiqi, High-efficiency measurement of an artificial atom embedded in a parametric amplifier, *Phys. Rev. X* **9**, 011004 (2019).
- [26] T. Yamamoto, K. Inomata, M. Watanabe, K. Matsuba, T. Miyazaki, W. D. Oliver, Y. Nakamura, and J. Tsai, Flux-driven Josephson parametric amplifier, *Appl. Phys. Lett.* **93**, 042510 (2008).
- [27] J. Aumentado, Superconducting parametric amplifiers: The state of the art in josephson parametric amplifiers, *IEEE Microw. Mag.* **21**, 45 (2020).
- [28] H. A. Haus and J. Mullen, Quantum noise in linear amplifiers, *Phys. Rev.* **128**, 2407 (1962).
- [29] M. Sandberg, C. Wilson, F. Persson, T. Bauch, G. Johansson, V. Shumeiko, T. Duty, and P. Delsing, Tuning the field in a microwave resonator faster than the photon lifetime, *Appl. Phys. Lett.* **92**, 203501 (2008).
- [30] N. Bergeal, F. Schackert, M. Metcalfe, R. Vijay, V. Manucharyan, L. Frunzio, D. Prober, R. Schoelkopf, S. Girvin, and M. Devoret, Phase-preserving amplification near the quantum limit with a Josephson ring modulator, *Nature* **465**, 64 (2010).
- [31] A. H. Nayfeh and D. T. Mook, *Nonlinear Oscillations* (John Wiley & Sons, New York, 2008).
- [32] Z. Lin, K. Inomata, K. Koshino, W. Oliver, Y. Nakamura, J.-S. Tsai, and T. Yamamoto, Josephson parametric phase-locked oscillator and its application to dispersive readout of superconducting qubits, *Nat. Commun.* **5**, 1 (2014).
- [33] P. Krantz, Y. Reshitnyk, W. Wustmann, J. Bylander, S. Gustavsson, W. D. Oliver, T. Duty, V. Shumeiko, and P. Delsing, Investigation of nonlinear effects in Josephson parametric oscillators used in circuit quantum electrodynamics, *New J. Phys.* **15**, 105002 (2013).
- [34] A. Bengtsson, P. Krantz, M. Simoen, I.-M. Svensson, B. Schneider, V. Shumeiko, P. Delsing, and J. Bylander, Non-degenerate parametric oscillations in a tunable superconducting resonator, *Phys. Rev. B* **97**, 144502 (2018).
- [35] C. H. Meaney, H. Nha, T. Duty, and G. J. Milburn, Quantum and classical nonlinear dynamics in a microwave cavity, *Eur. Phys. J. Quantum Technol.* **1**, 1 (2014).

- [36] W. Wustmann and V. Shumeiko, Parametric resonance in tunable superconducting cavities, *Phys. Rev. B* **87**, 184501 (2013).
- [37] H. Goto, Bifurcation-based adiabatic quantum computation with a nonlinear oscillator network, *Sci. Rep.* **6**, 21686 (2016).
- [38] H. Goto, Universal quantum computation with a nonlinear oscillator network, *Phys. Rev. A* **93**, 050301 (2016).
- [39] S. Puri, S. Boutin, and A. Blais, Engineering the quantum states of light in a kerr-nonlinear resonator by two-photon driving, *npj Quantum Inf.* **3**, 1 (2017).
- [40] M. Mirrahimi, Z. Leghtas, V. V. Albert, S. Touzard, R. J. Schoelkopf, L. Jiang, and M. H. Devoret, Dynamically protected cat-qubits: A new paradigm for universal quantum computation, *New J. Phys.* **16**, 045014 (2014).
- [41] P. Krantz, A. Bengtsson, M. Simoen, S. Gustavsson, V. Shumeiko, W. Oliver, C. Wilson, P. Delsing, and J. Bylander, Single-shot read-out of a superconducting qubit using a Josephson parametric oscillator, *Nat. Commun.* **7**, 11417 (2016).
- [42] C. Wilson, T. Duty, M. Sandberg, F. Persson, V. Shumeiko, and P. Delsing, Photon Generation in an Electromagnetic Cavity With a Time-Dependent Boundary, *Phys. Rev. Lett.* **105**, 233907 (2010).
- [43] B. Yurke, R. Movshovich, P. Kaminsky, P. Bryant, A. Smith, A. Silver, and R. Simon, Behavior of noise in a non-degenerate Josephson-parametric amplifier, *IEEE Trans. Magn.* **27**, 3374 (1991).
- [44] M. Reid and B. Yurke, Effect of bistability and superpositions on quantum statistics in degenerate parametric oscillation, *Phys. Rev. A* **46**, 4131 (1992).
- [45] H. Olsson and T. Claeson, Low-noise Josephson parametric amplification and oscillations at 9 GHz, *J. Appl. Phys.* **64**, 5234 (1988).
- [46] A. Hajimiri and T. H. Lee, A general theory of phase noise in electrical oscillators, *IEEE J. Solid-State Circuits* **33**, 179 (1998).
- [47] A. Demir, A. Mehrotra, and J. Roychowdhury, Phase noise in oscillators: A unifying theory and numerical methods for characterization, *IEEE Trans. Circuits Syst. Fundam. Theory Appl.* **47**, 655 (2000).
- [48] G. Sauvage, Phase noise in oscillators: A mathematical analysis of Leeson's model, *IEEE Trans. Instrum. Meas.* **26**, 408 (1977).
- [49] S. Reynaud, C. Fabre, and E. Giacobino, Quantum fluctuations in a two-mode parametric oscillator, *JOSA B* **4**, 1520 (1987).
- [50] J. Courtois, A. Smith, C. Fabre, and S. Reynaud, Phase diffusion and quantum noise in the optical parametric oscillator: a semiclassical approach, *J. Mod. Opt.* **38**, 177 (1991).
- [51] C. Henry, Theory of the phase noise and power spectrum of a single mode injection laser, *IEEE J. Quantum Electron.* **19**, 1391 (1983).
- [52] T. Debuisschert, S. Reynaud, A. Heidmann, E. Giacobino, and C. Fabre, Observation of large quantum noise reduction using an optical parametric oscillator, *Quantum Opt.* **1**, 3 (1989).
- [53] Z. Lin, Y. Nakamura, and M. Dykman, Critical fluctuations and the rates of interstate switching near the excitation threshold of a quantum parametric oscillator, *Phys. Rev. E* **92**, 022105 (2015).
- [54] E. Hinkley and C. Freed, Direct Observation of the Lorentzian Line Shape as Limited by Quantum Phase Noise in a Laser Above Threshold, *Phys. Rev. Lett.* **23**, 277 (1969).
- [55] L. Frunzio, A. Wallraff, D. Schuster, J. Majer, and R. Schoelkopf, Fabrication and characterization of superconducting circuit QED devices for quantum computation, *IEEE Trans. Appl. Supercond.* **15**, 860 (2005).
- [56] H. Haken, Cooperative phenomena in systems far from thermal equilibrium and in nonphysical systems, *Rev. Mod. Phys.* **47**, 67 (1975).
- [57] W. Wustmann and V. Shumeiko, Parametric effects in circuit quantum electrodynamics, *Low Temp. Phys.* **45**, 848 (2019).
- [58] M. Dykman, *Fluctuating Nonlinear Oscillators: from Nanomechanics to Quantum Superconducting Circuits* (Oxford University Press, Oxford, 2012).
- [59] J. Gao, J. Zmuidzinas, B. A. Mazin, H. G. LeDuc, and P. K. Day, Noise properties of superconducting coplanar waveguide microwave resonators, *Appl. Phys. Lett.* **90**, 102507 (2007).
- [60] J. Gao, L. Vale, J. Mates, D. Schmidt, G. Hilton, K. Irwin, F. Mallet, M. Castellanos-Beltran, K. Lehnert, and J. Zmuidzinas, *et al.*, Strongly quadrature-dependent noise in superconducting microresonators measured at the vacuum-noise limit, *Appl. Phys. Lett.* **98**, 232508 (2011).
- [61] P. Welch, The use of fast Fourier transform for the estimation of power spectra: A method based on time averaging over short, modified periodograms, *IEEE Trans. Audio Electroacoust.* **15**, 70 (1967).
- [62] R. C. Dugan, M. F. McGranaghan, and H. W. Beaty, *Electrical Power Systems Quality* (McGraw-Hill, New York, 2002).
- [63] M. Tahir and S. K. Mazumder, Improving dynamic response of active harmonic compensator using digital comb filter, *IEEE Trans. Emerg. Sel. Topics Power Electron.* **2**, 994 (2014).
- [64] S. Machlup, Noise in semiconductors: spectrum of a two-parameter random signal, *J. Appl. Phys.* **25**, 341 (1954).
- [65] X. Pan, Y. Zhou, H. Yuan, L. Nie, W. Wei, L. Zhang, J. Li, S. Liu, Z. H. Jiang, and G. Catelani, *et al.*, Engineering superconducting qubits to reduce quasiparticles and charge noise, *Nat. Commun.* **13**, 1 (2022).
- [66] J. R. Friedman and S. Han, Exploring the quantum/classical frontier: recent advances in macroscopic quantum phenomena, (2003).
- [67] M. Razavy, *Quantum Theory of Tunneling* (World Scientific, River Edge, New Jersey, 2013).
- [68] M. Dykman, Critical exponents in metastable decay via quantum activation, *Phys. Rev. E* **75**, 011101 (2007).
- [69] M. H. Devoret, J. M. Martinis, and J. Clarke, Measurements of Macroscopic Quantum Tunneling Out of the Zero-Voltage State of a Current-Biased Josephson Junction, *Phys. Rev. Lett.* **55**, 1908 (1985).
- [70] D. Marković, J.-D. Pillet, E. Flurin, N. Roch, and B. Huard, Injection Locking and Parametric Locking in a Superconducting Circuit, *Phys. Rev. Appl.* **12**, 024034 (2019).